



Planetary Crater Detection and Registration Using Marked Point Processes, Graph Cut Algorithms, and Wavelet Transforms

Authors: Alberto Gotelli², Gabriele Moser²,
Jacqueline Le Moigne¹, and Sebastiano B. Serpico²

¹ NASA Goddard Space Flight Center

² University of Genoa





Contents



- Introduction
- Proposed methodology
 - Marked point processes for crater modeling
 - Multiple birth and cut for crater detection
 - Image registration
 - Wavelet decomposition
- Experimental results
 - Crater detection results
 - Registration results on semi-synthetic data
 - Registration results on real data
- Conclusion and future developments





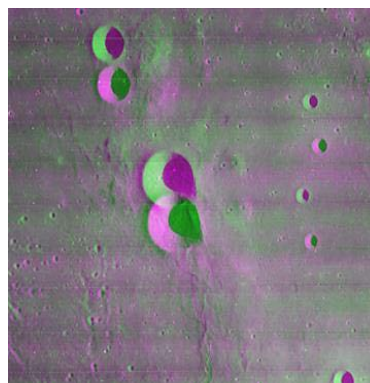
Contents



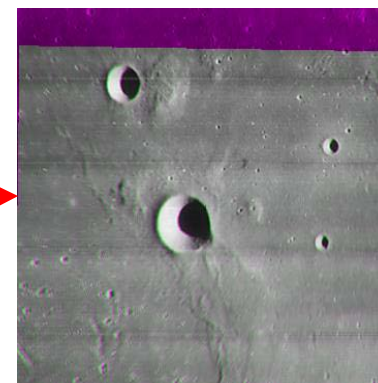
- Introduction
- Proposed methodology
 - Marked point processes for crater modeling
 - Multiple birth and cut for crater detection
 - Image registration
 - Wavelet decomposition
- Experimental results
 - Crater detection results
 - Registration results on semi-synthetic data
 - Registration results on real data
- Conclusion and future developments



- Process of **aligning two or more planetary images**, or one or more images wrt another data source
- **Fundamental task** for using multiple images (often coming from diverse missions) for planetary science applications
- **Challenging task** because of possibly large differences between the acquired images, of their possibly heterogeneous nature (e.g., multisensor), and of their size



Before registration



After registration



Overview



Objectives

- Proposing a new approach for planetary image **registration**
- Extracting **craters** (especially large ones) to be used for registration
- Validating the approach with real planetary/lunar data

Key Ideas

- Using a **marked point process** model coupled with a **multiple birth and cut** algorithm for crater extraction
- Using the extracted craters to obtain a **preliminary registration**
- Maximizing **mutual information** within the image pair in a neighborhood of the preliminary transformation to minimize error





Contents

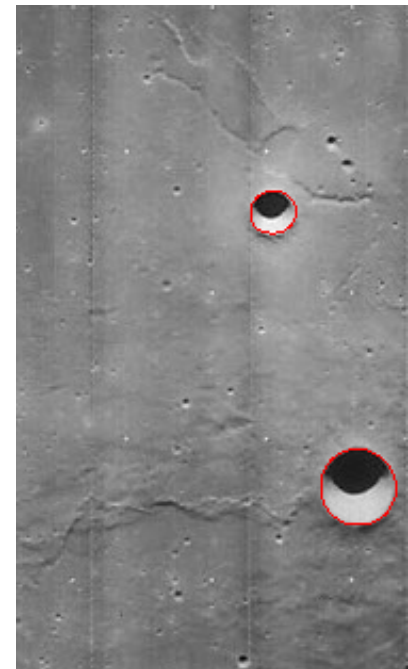


- Introduction
- **Proposed methodology**
 - Marked point processes for crater modeling
 - Multiple birth and cut for crater detection
 - Image registration
 - Wavelet decomposition
- Experimental results
 - Crater detection results
 - Registration results on semi-synthetic data
 - Registration results on real data
- Conclusion and future developments



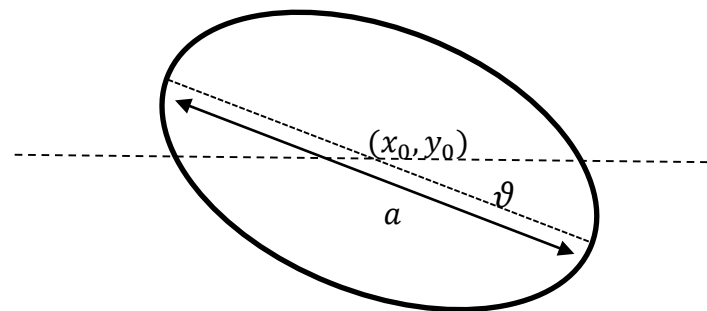
Marked point processes

- A **point process** is a stochastic process whose realizations are sets of points in the image plane (e.g. Poisson points).
- In an **MPP**, each point is enriched with additional variables (**marks**) that parameterize an object attached to the point.
- Flexible and powerful models for simultaneous detection of an **unknown number of parameterized objects**
- Markov properties allows modeling local interactions and defining a prior on the object distribution in the scene



MPP for craters: ellipse with low eccentricity

- Orientation angle ϑ
- Center coordinates (x_0, y_0)
- Major axis a
- Eccentricity e





Crater Extraction – Energy Function



- Bayesian estimation of the configuration $X = \{x_i\}_{i=1}^n$ of ellipses given image data (Canny contour map C): energy minimization

$$p(X|C) \propto e^{-U(X|C)} \quad U(X|C) = U_P(X) + U_L(C|X)$$

- Prior penalizes overlapping ellipses in the scene

$$U_P(X) = \frac{1}{n} \sum_{x_i \wedge x_j > 0} R_{ij} \quad \text{where} \quad R_{ij} = \begin{cases} \frac{x_i \wedge x_j}{x_i \vee x_j} & \text{for } \frac{x_i \wedge x_j}{x_i \vee x_j} \leq 0.1 \\ 1 & \text{otherwise} \end{cases}$$

$x_i \vee x_j$ = area of union of ellipses x_i and x_j

$x_i \wedge x_j$ = area of intersection of x_i and x_j



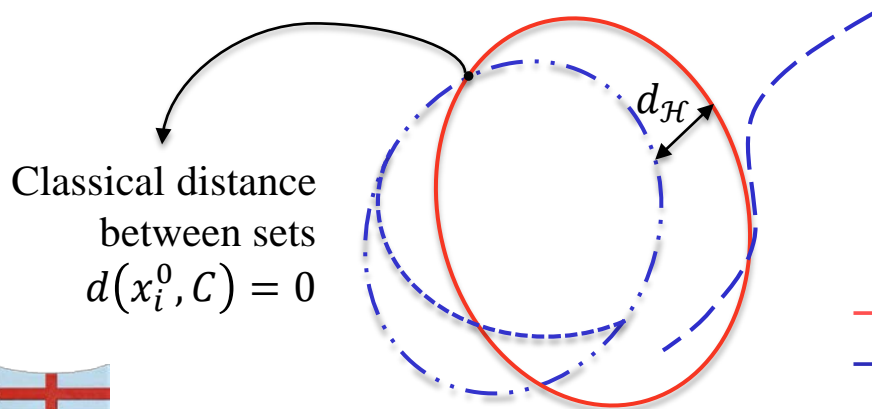
- Likelihood** favors the fit between contours and ellipses through a correlation measure and a Hausdorff distance measure:

$$U(X|C) = U_P(X) + U_L(C|X) \quad U_L(C|X) = \sum_{i=1}^n \left[\frac{d_{\mathcal{H}}(x_i^0, C)}{na_i} - \frac{|x_i^0 \cap C|}{|x_i^r \cap C|} \right]$$

x_i^0 = set of pixels associated with ellipse x_i in the image

x_i^r = set of pixels inside an annulus of radius r around ellipse x_i

$d_{\mathcal{H}}(x_i^0, C)$ = Hausdorff distance between x_i and contours



$$d_{\mathcal{H}}(A, B) = \max \left\{ \sup_{\alpha \in A} \inf_{\beta \in B} d(\alpha, \beta); \sup_{\beta \in B} \inf_{\alpha \in A} d(\alpha, \beta) \right\}$$



Crater Extraction – MBC



Multiple Birth and Cut (MBC): algorithm for MPP energy minimization proposed within Earth observation applications

1. Initialization: $n \leftarrow 0$, $R \leftarrow \text{constant}$

2. Generate a new configuration $X_{(0)}$

3. **Repeat:**

4. Birth: generate X' composed of R new non-overlapping ellipses

5. $X'' \leftarrow X_{(n)} \cup X'$: all candidate ellipses

6. Cut: classify X'' between craters to be kept and those to be discarded using graph cuts on a case-specific graph associated with the energy contributions
 $\Rightarrow X_{(n+1)}$ is obtained

7. **Until** convergence is reached





Image Registration – First Step



- Rotation Scale and Translation (RST) transform T_p , parameterized by $p = (t_x, t_y, \vartheta, k)$
- **First registration step**
 - **Craters** x_i^{ref} ($i = 1, 2, \dots, n$) are extracted from reference image.
 - Transformation T_p is applied to **contours** C^{in} of input image.
 - **Fit** between transformed contours $T_p(C^{in})$ and craters is evaluated:

$$\mathcal{J}(p) = \sum_{i=1}^n \left[\frac{d_{\mathcal{H}}(x_i^{ref}, T_p(C^{in}))}{na_i^{ref}} - \frac{|x_i^{ref} \cap T_p(C^{in})|}{|T_p(C^{in})|} \right]$$

- $\mathcal{J}(p)$ is minimized through **generalized pattern search** (with search phase based on a genetic algorithm)





Image Registration – Second Step



- Second registration step

- Max **mutual information** in a neighborhood of the transformation resulting from the first step (to obtain higher accuracy)
- Mutual information between two discrete variables Y and Z :

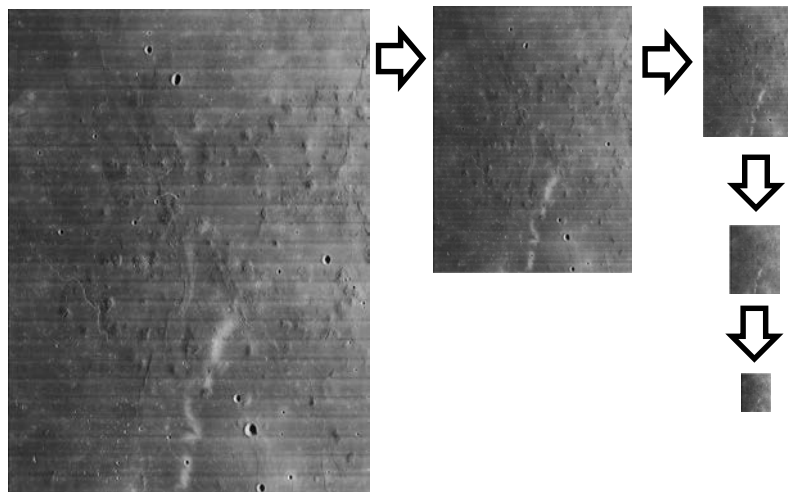
$$I(Y, Z) = \sum_y \sum_z P(y, z) \log \left(\frac{P(y, z)}{P(y)P(z)} \right)$$

- Mutual information $I(p)$ between input image transformed by 1st step and reference image is evaluated as a function of a further transformation p , estimating probabilities through histograms.
- $I(p)$ is maximized using simulated annealing.



Crater detection is generally time-consuming: **wavelets** to speed up the process and incorporate multiscale information.

- **Decimated wavelets** are applied to reference and input images keeping only the LL components.
- **Hierarchical** crater detection and registration **from coarsest to finest scale**
- From each scale to the next, transformation is adapted and refined in a neighborhood, and regions where craters are detected are removed to minimize computational burden.





Contents



- Introduction
- Proposed methodology
 - Marked point processes for crater modeling
 - Multiple birth and cut for crater detection
 - Image registration
 - Wavelet decomposition
- **Experimental results**
 - Crater detection results
 - Registration results on semi-synthetic data
 - Registration results on real data
- Conclusion and future developments

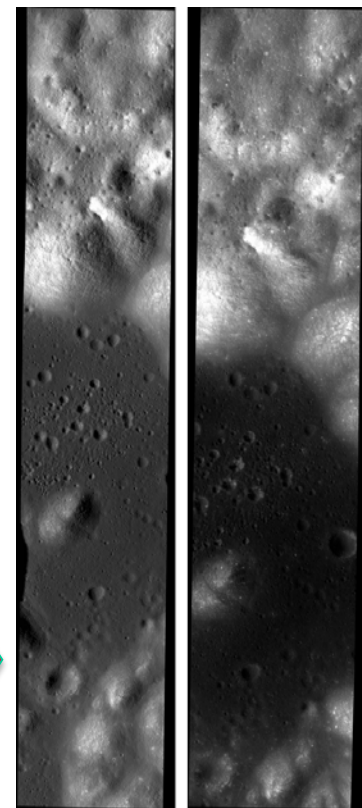
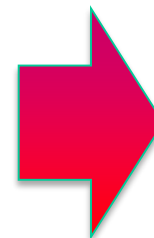


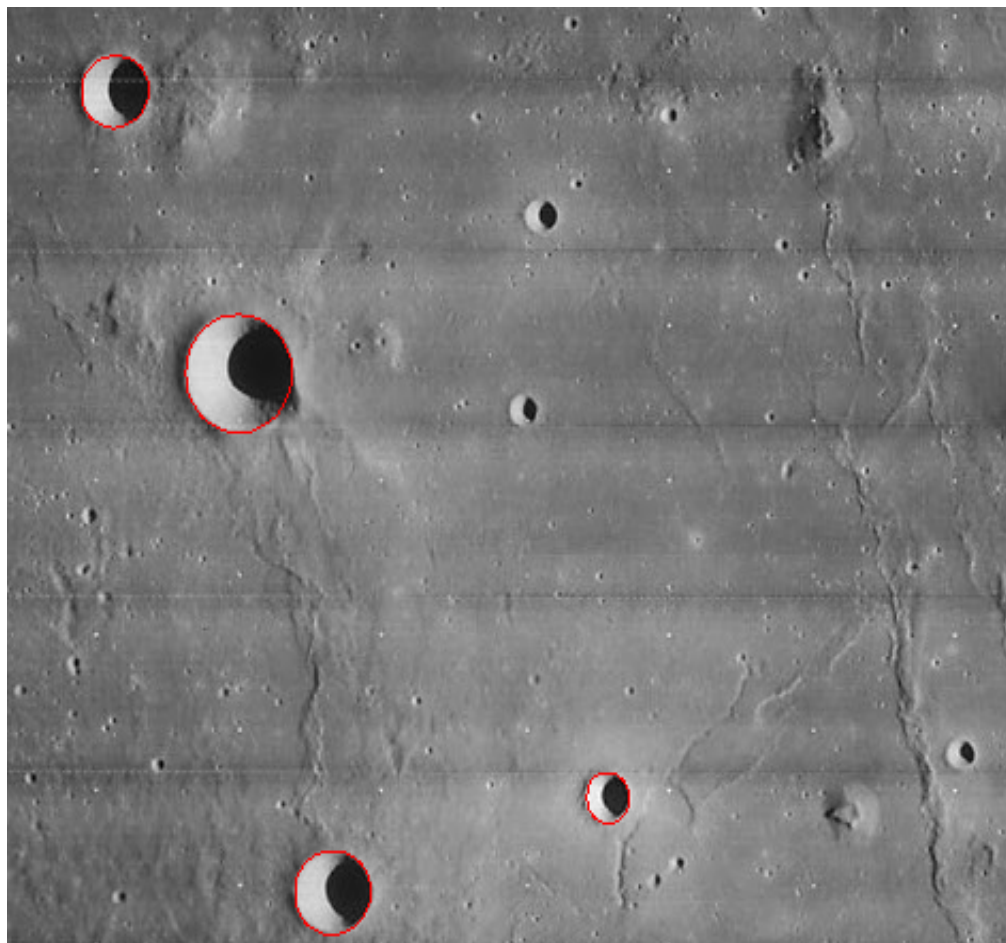
To validate crater detection results

- 6 THEMIS (Thermal Emission Imaging System) images, TIR, 100m resolution, Mars Odyssey mission
- 7 HRSC (High Resolution Stereo Color) images, VIS, ~20m resolution, Mars Express mission
- Image sizes from 1581×1827 to 2950×5742 pixels

To validate registration results

- Semi-simulated image pairs: 20 pairs composed of one real THEMIS or HRSC image and of an image obtained by applying a synthetic transform and AWGN ► *quantitative validation wrt true transform*
- Real multitemporal pair of LROC (Lunar Reconnaissance Orbiter Camera) images, 100m resolution ► *qualitative visual analysis*

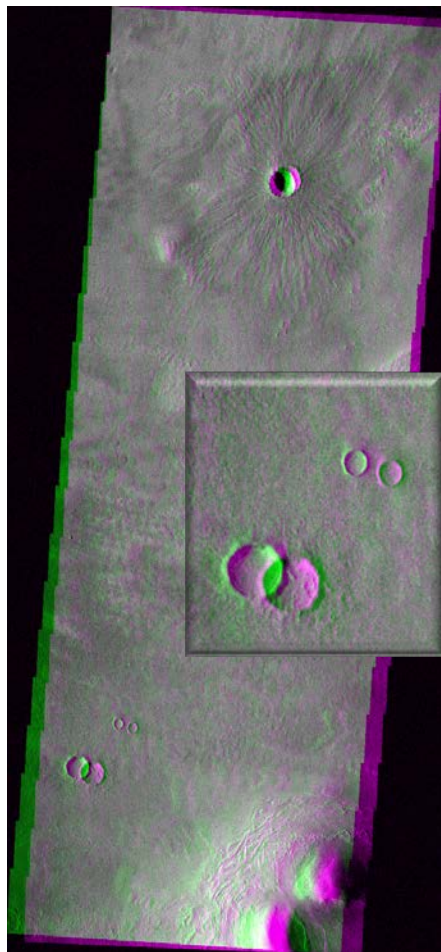




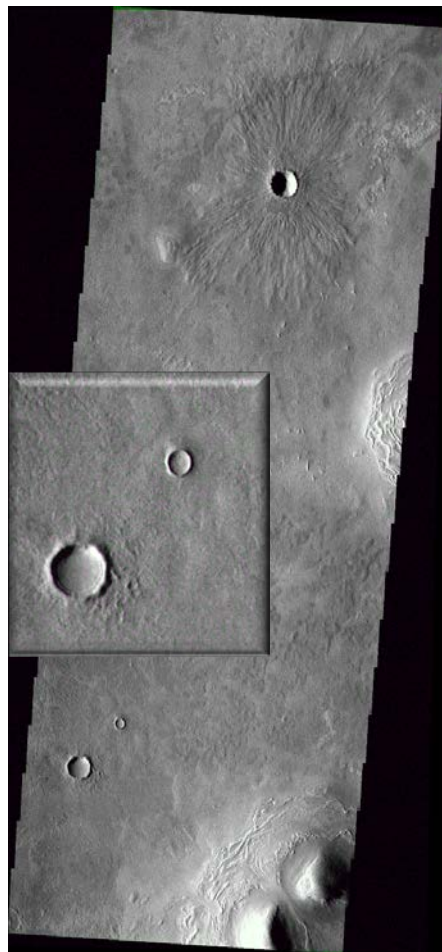
- Visually precise detection
- Focus on large craters: **missed alarms** correspond to small craters, which are much less relevant than large craters for registration.
- No false alarms in any of the considered images
- Detection percentage D :
 - Average on THEMIS: **0.82**
 - Average on HRSC: **0.74**
 - Average on all images: **0.78**

$$D = \frac{TP}{TP + FN}$$

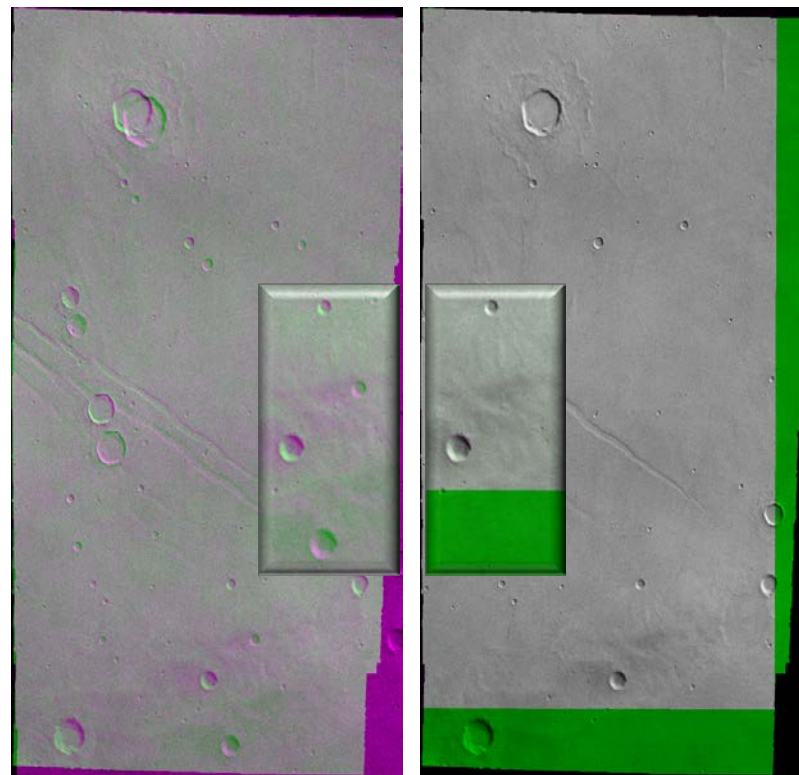
RGB composites of reference and input images



Before registration



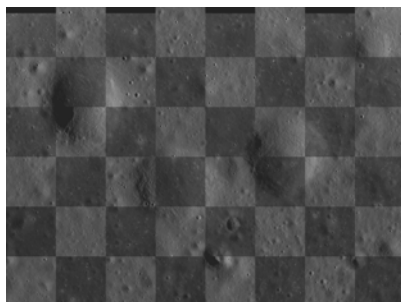
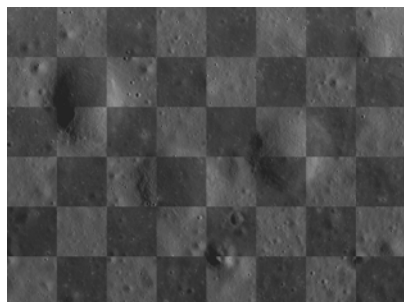
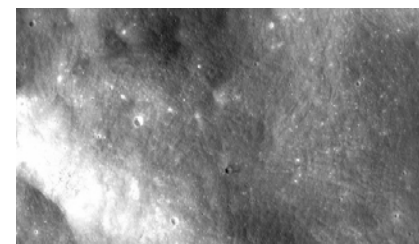
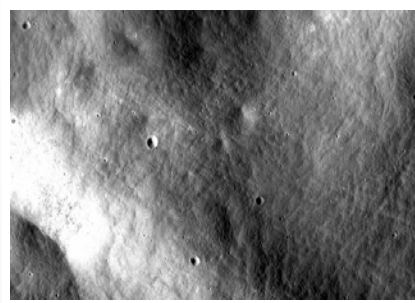
After registration



Visually accurate registration

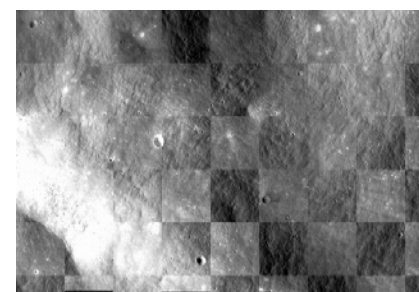
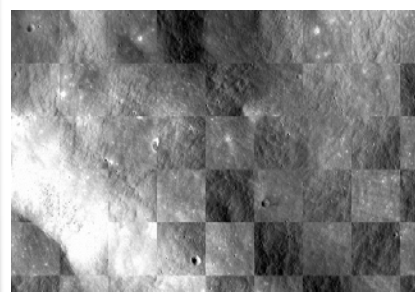
Subpixel RMS registration error:

- Avg on 10 THEMIS pairs: **0.54** pixel
- Avg on 10 HRSC pairs: **0.59** pixel
- Avg on all 20 pairs: **0.57** pixel



Before registration

After registration



Before registration

After registration

Two crops of the original images and their checkerboard representation are reported before and after registration: **visually accurate registration**.

Ground truth is not available for quantitative assessment so this representation is used as a simple way to qualitatively evaluate the results.



Contents



- Introduction
- Proposed methodology
 - Marked point processes for crater modeling
 - Multiple birth and cut for crater detection
 - Image registration
 - Wavelet decomposition
- Experimental results
 - Crater detection results
 - Registration results on semi-synthetic data
 - Registration results on real data
- Conclusion and future developments





Conclusions and Future Development



Conclusion

- The proposed MPP-MBC approach proved effective for crater extraction from planetary/lunar images.
- The developed 2-step registration approach was effective and rather fast (max a few tens of minutes for max $\sim 3000 \times 6000$ pixels).
- Visually accurate registration results from real multitemporal images with rather large differences in illumination.

Future Developments

- Extension to multisensor and multiresolution images
- Parallelized more efficient implementations.





Main Bibliography



- J. Le Moigne, N. S. Netanyahu and R. Eastman, Image Registration for Remote Sensing, Cambridge: Cambridge University Press, 2011.
- I. Zavorin and J. Le Moigne, "Use of Multiresolution Wavelet Feature Pyramids for Automatic Registration of Multisensor Imagery," IEEE Transaction on Image Processing, vol. 14, no. 6, 2005.
- G. Troglia, J. A. Benediktsson, G. Moser and S. B. Serpico, "Crater Detection Based on Marked Point Processes," in Signal and Image Processing for Remote Sensing, Boca Raton, FL, CRC Press, 2012, pp. 325-338.
- X. Descombes and J. Zerubia, "Marked point processes in image analysis," IEEE Signal Processing Magazine, vol. 19, no. 5, pp. 77-84, 2002.
- J. M. Murphy, J. Le Moigne and D. J. Harding, "Automatic Image Registration of Multimodal Remotely Sensed Data With Global Shearlet Features," IEEE Transactions on Geoscience and Remote Sensing, vol. 54, no. 3, pp. 1685-1704, 2016.
- A. Gamal-Eldin, X. Descombes and J. Zerubia, "Multiple Birth and Cut Algorithm for Point Process Optimization," Signal-Image Technology and Internet-Based Systems (SITIS), 2010 Sixth International Conference, pp. 33-42, 2010.
- A. Gamal-Eldin, X. Descombes, G. Charpiat and J. Zerubia, "A fast Multiple Birth and Cut algorithm using belief propagation," IEEE International Conference on Image Processing, pp. 2813-2816, 2011.
- Y. Boykov and V. Kolmogorov, "An Experimental Comparison of Min-Cut/Max-Flow Algorithms for Energy Minimization in Vision," IEEE Transactions on PAMI, vol. 26, no. 9, pp. 1124-1137, 2004.





Appendix





RST Transformation



- Transformation with four parameters, i.e. two of translation, one of scaling, and one of rotation
- Can be defined through a matrix T that maps the image coordinates to new ones according to the four parameters:

$$T: (x, y, 1) \mapsto (x', y')$$

with:

$$T = \begin{bmatrix} k \cos \vartheta & k \sin \vartheta & t_x \\ -k \sin \vartheta & k \cos \vartheta & t_y \\ 0 & 0 & 1 \end{bmatrix}$$

- $p = [t_x \quad t_y \quad k \quad \vartheta]$ is the transformation vector that defines the translation, the scaling factor, and the rotation.





GPS Algorithm



- Flexible class of derivative-free unconstrained optimization algorithms
- Nicely fit the computation of p because $\mathcal{J}(p)$ is generally non-differentiable.

- Mesh Creation with the *GPS Positive Basis 2N* method
- Combination of these vectors with the mesh size and the current point gives the new points to be tested.
- *Search phase*: a genetic algorithm searches in the mesh for a point with a lower value of \mathcal{J} than the current point.
- *Poll phase*: before declaring an iteration unsuccessful, the neighboring mesh points are polled for points with a lower value of \mathcal{J} .

- **Initialization**

Let $x_0 \in \Gamma$ be such that $f(x_0)$ is finite, and let M_0 be a mesh on \mathbb{R}^n

- **Search and Poll Steps**

Perform the search and the poll steps until a trial point x_{k+1} with a lower objective function value is found, or when it is shown that no such trial point exists

Search Step: Evaluate the objective function on a finite subset of feasible trial points on the mesh M_k

Poll step: Evaluate the objective function on the poll set around x_k

- **Parameter Update**

If the search or the poll step produced a feasible iterate $x_{k+1} \in M_k \cap \Gamma$ for which $f(x_{k+1}) < f(x_k)$, then declare the iteration successful and increase the mesh size. Otherwise, decrease the mesh size if the iteration was unsuccessful.





Image Registration – RMS



- When an accurate ground truth is available, the RMS registration error can be computed analytically.

- Error transf. $p_\epsilon = (t_{x_\epsilon}, t_{y_\epsilon}, \vartheta_\epsilon, k_\epsilon)$
- GT transf. $p_{GT} = (t_{x_1}, t_{y_1}, \vartheta_1, k_1)$
- Computed transf. $p = (t_{x_2}, t_{y_2}, \vartheta_2, k_2)$
- $Q_{p_\epsilon} = Q_p Q_{p_{GT}}^{-1}$
- $k_\epsilon = \frac{k_2}{k_1}, \quad \vartheta_\epsilon = \vartheta_2 - \vartheta_1$
- $t_{x_\epsilon} = t_{x_2} - k_\epsilon(t_{x_1} \cos \vartheta_\epsilon + t_{y_1} \sin \vartheta_\epsilon)$
- $t_{y_\epsilon} = t_{y_2} - k_\epsilon(t_{y_1} \cos \vartheta_\epsilon - t_{x_1} \sin \vartheta_\epsilon)$
- $\begin{bmatrix} x' \\ y' \end{bmatrix} = k_\epsilon \begin{pmatrix} \cos \vartheta_\epsilon & \sin \vartheta_\epsilon \\ -\sin \vartheta_\epsilon & \cos \vartheta_\epsilon \end{pmatrix} \begin{bmatrix} x \\ y \end{bmatrix} + \begin{bmatrix} t_{x_\epsilon} \\ t_{y_\epsilon} \end{bmatrix}$

$$E(p_\epsilon) = \sqrt{\frac{1}{AB} \int_0^A \int_0^B (x' - x)^2 + (y' - y)^2 dx dy}$$

$$E^2(p_\epsilon) = \frac{\alpha}{3} (k_\epsilon^2 - 2k_\epsilon \cos \vartheta_\epsilon + 1) + (t_{x_\epsilon}^2 + t_{y_\epsilon}^2) - (At_{x_\epsilon} + Bt_{y_\epsilon})(1 - k_\epsilon \cos \vartheta_\epsilon) - k_\epsilon (At_{y_\epsilon} - Bt_{x_\epsilon}) \sin \vartheta_\epsilon$$





Crater Extraction (4) - MBC



Multiple Birth and Cut: algorithm for MPP energy minimization proposed within Earth observation applications

1. Initialization: $n \leftarrow 0$, $R \leftarrow \text{constant}$
2. Generate a new configuration $\omega', \omega_{(0)} \leftarrow \omega'$
3. **Repeat:**
4. Birth: generate ω''
5. $\omega_{(n+1)} \leftarrow \omega_{(n)} \cup \omega'' \rightarrow \text{Graph Construction}$
6. Cut: optimize with graph cuts
7. **Until** convergence is reached

Convergence:

Here the convergence is considered to be reached when the cut returns the same configuration of objects for many consecutive iterations.



Multiple Birth and Cut: algorithm for MPP energy minimization proposed within Earth observation applications

1. Initialization: $n \leftarrow 0$, $R \leftarrow \text{constant}$
2. Generate a new configuration ω' , $\omega_{(0)} \leftarrow \omega'$
3. **Repeat:**
4. Birth: generate ω''
5. $\omega_{(n+1)} \leftarrow \omega_{(n)} \cup \omega'' \rightarrow \text{Graph Construction}$
6. Cut: optimize with graph cuts
7. **Until** convergence is reached

Example ($R = 1$):

